ISSN 1330-3651 (Print), ISSN 1848-6339 (Online)
Received: 11 November 2025; Accepted: 26 January 2026

https://doi.org/10.17559/TV-20251111003125
Original scientific paper

Adaptive Threshold Algorithms for Energy Optimization in LoRa-Based Air Quality Monitoring Networks

Ljubomir VRAČAR, Jonas MATIJOŠIUS, Milan STOJANOVIĆ, Artūras KILIKEVIČIUS, Miloš MILOVANČEVIĆ*

Abstract This paper presents the design and evaluation of an energy-efficient multisensor platform for air-quality monitoring based on LoRa communication and the TEEN routing protocol. The system integrates a low-power PIC18F45K22 microcontroller, SPEC electrochemical sensors for CO and NO_2 detection, and an LMP91000 analog front-end, powered by a photovoltaic energy-harvesting subsystem. The proposed architecture employs adaptive, threshold-based algorithms to minimize the frequency of wireless data transmissions while maintaining high measurement accuracy. Four transmission strategies were implemented and tested to evaluate the trade-off between data fidelity and energy efficiency. Experimental validation was performed at the archaeological site Mediana (Niš, Serbia), where the system continuously measured temperature, humidity, and pollutant concentrations over seven days. Results demonstrate that the event-driven transmission method achieved correlation coefficients above 0.99 with an 85 % reduction in total energy consumption compared to continuous transmission. The findings confirm that integrating LoRa communication with TEEN-based routing provides a robust and sustainable framework for long-term environmental monitoring. The proposed platform offers scalability, autonomy, and low operational cost, making it suitable for next-generation IoT-based smart-city air-quality networks.

Keywords: air quality; energy efficiency; environmental monitoring; IoT; LoRa; TEEN protocol; wireless sensor network

1 INTRODUCTION

Air pollution represents one of the most pressing environmental and public health issues of the twenty-first century. Numerous studies have confirmed a strong correlation between long-term exposure to airborne pollutants and the increased incidence of respiratory and cardiovascular diseases. Continuous air-quality monitoring is therefore essential for effective environmental management and regulatory control [1]. However, conventional monitoring stations are expensive, bulky, and complex to maintain, which significantly limits their spatial coverage and responsiveness in urban and industrial areas.

Recent advances in Wireless Sensor Networks (WSNs) have enabled low-cost, scalable, and flexible solutions for environmental monitoring. WSNs consist of distributed sensor nodes capable of measuring temperature, humidity, and concentrations of gases such as CO, CO_2, NO_2, and O_3, transmitting data wirelessly to a central node or cloud platform [2]. Despite these advantages, WSN-based systems continue to face substantial challenges related to energy efficiency, communication range, environmental adaptability, and operational reliability under diverse outdoor conditions.

To overcome these constraints, recent research efforts have focused on the development of energy-efficient communication protocols and low-power transmission methods. Among them, LoRa (Long Range) technology stands out due to its ability to facilitate long-distance, low-energy data exchange over several kilometers [3]. When integrated with adaptive routing schemes such as the Threshold-sensitive Energy Efficient Network (TEEN) protocol, LoRa-based WSNs can drastically reduce redundant data transmissions. This event-driven approach ensures that sensor nodes transmit only when significant environmental variations are detected, thereby conserving energy while preserving measurement accuracy [4, 5].

Building on these principles, the present study introduces a multisensor IoT platform specifically engineered for low-power air quality monitoring. The system employs TEEN-enhanced LoRa communication technology to ensure ultra-low-power operation across a wide range of environmental conditions. The platform is capable of collecting essential data such as concentrations of gases CO and NO_2, temperature, and relative humidity. By implementing adaptive, threshold-based transmission intervals ranging from 4 to 60 minutes, the system intelligently balances data resolution and power consumption, achieving a notable wireless operational range exceeding 1.5 km [6, 7].

The integration of TEEN with LoRa not only optimizes communication efficiency but also significantly improves the overall energy performance of the network. As a result, the proposed system demonstrates a longer operational lifetime and reduced maintenance requirements compared to traditional Frequency Shift Keying (FSK)-based approaches. Furthermore, the proposed design shows strong compatibility with smart city frameworks and environmental IoT infrastructures, making it suitable for large-scale deployment [8].

Previous research initiatives have documented successful air quality monitoring implementations utilizing particulate matter sensors in dense urban environments [9, 10]. The methodology presented in this paper builds upon and extends these foundations by introducing a more sustainable and power-efficient communication framework. Consequently, the system represents a sustainable foundation for next-generation IoT-based environmental monitoring, ensuring enhanced scalability, accuracy, and adaptability in both urban and rural contexts.

While the algorithmic approaches used in this research build upon well-known TEEN-based transmission control methods, the key innovation of this study is the determination of specific boundary thresholds that achieve an optimal balance between energy consumption and signal reconstruction accuracy. Instead of relying on generic or theoretically assumed parameters, the paper introduces experimentally validated threshold values that significantly enhance system performance in realistic outdoor monitoring scenarios.

2 HARDWARE ARCHITECTURE

The proposed air-quality monitoring platform was designed as a compact, energy-efficient, and modular system optimized for long-term outdoor operation. The hardware architecture integrates a microcontroller-based control unit, a digital temperature and humidity sensor, a dual electrochemical gas-sensing stage, a LoRa radio communication module, and an autonomous photovoltaic power subsystem, as shown in Fig 1.

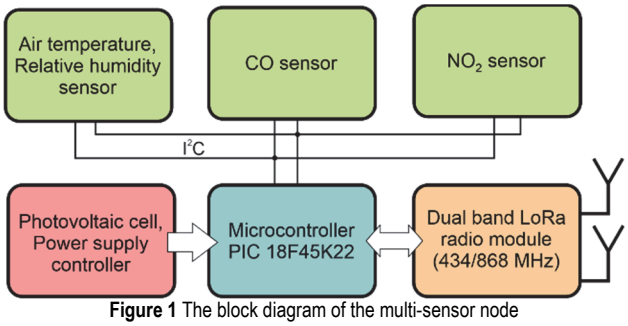

Figure 1 The block diagram of the multi-sensor node

At the core of the system is the PIC18F45K22 microcontroller, selected for its low power consumption, integrated analog-to-digital conversion capabilities, and sufficient computational performance for real-time data acquisition and transmission control [11]. The microcontroller operates as the central processing and coordination unit, managing sensor readings, digital communication via the I²C bus, and timing of LoRa data transmissions.

The temperature and relative humidity were measured by the Honeywell HIH-6100 series digital sensor [12]. It operates over a wide voltage and temperature range, offers a low power consumption and high humidity accuracy.

For pollutant detection, two electrochemical gas sensors manufactured by SPEC Sensors Inc. were employed:

- 3SP_NO2_20, for measuring nitrogen dioxide (NO_2) concentrations [13], and
- 3SP_CO_1000, for carbon monoxide (CO) detection [14].

Both sensors offer high sensitivity and stability for ambient air-quality applications. To optimize signal conditioning and simplify hardware design, both sensors are connected through the LMP91000 [15] analog front-end IC (Texas Instruments). This programmable potentiostat serves as an interface between the electrochemical sensor and the microcontroller, providing configurable transimpedance amplification, bias control, and internal reference voltages. Communication between the LMP91000 and the PIC18F45K22 microcontroller is realized through the I²C serial interface, enabling flexible digital configuration and calibration of sensing parameters. The use of the LMP91000 significantly reduces the need for external analog circuitry and contributes to overall system miniaturization.

For long-range wireless data transmission, the system employs a LoRa radio transceiver module operating in dual-band 434/868 MHz mode. This configuration ensures compatibility with both European and global sub-GHz ISM frequency bands, allowing the device to operate within LoRaWAN infrastructures or standalone point-to-point links. LoRa technology was chosen for its low power demand, extended communication range (up to several kilometers in line-of-sight conditions), and robustness in urban environments.

The device is designed for autonomous field deployment and thus powered by a photovoltaic energy-harvesting subsystem. A compact solar cell continuously charges a lithium-ion battery through an integrated charging controller, ensuring uninterrupted operation during low-light conditions or at night. The power-management circuit includes voltage regulation and low-dropout conversion stages to maintain stable supply voltages for both analog and digital components. This hybrid power solution enables the system to sustain long-term monitoring without the need for manual recharging or external grid connection.

Overall, the hardware design provides a reliable and autonomous low-power platform. The combination of LoRa connectivity and the LMP91000 interface ensures accurate measurements, minimal energy consumption, and adaptability for scalable environmental monitoring applications.

3 COMMUNICATION FRAMEWORK AND ENERGY OPTIMIZATION

Energy consumption during wireless data transmission represents one of the most critical constraints in the design of low-power environmental monitoring systems. In a typical wireless sensor node, a substantial portion of the total energy budget is expended during the transmission phase. Although LoRa modulation inherently provides a significant reduction in power consumption due to its long-range and low-data-rate characteristics, further optimization is required to minimize the number of transmissions while maintaining adequate measurement accuracy [16, 17].

To address this challenge, the present system integrates the Threshold-sensitive Energy Efficient Sensor Network (TEEN) routing protocol. TEEN is a hierarchical, event-driven communication scheme designed to reduce unnecessary data transmissions by allowing nodes to remain inactive until meaningful environmental changes occur [18]. Compared to traditional protocols such as LEACH or PEGASIS [19], TEEN achieves superior energy efficiency by combining local data evaluation with conditional transmission activation [20]. This structure enables both multi-hop communication among nodes and direct communication to the gateway, depending on network configuration. Consequently, the protocol efficiently balances energy consumption across the network while preserving real-time responsiveness for critical environmental events.

The TEEN protocol operates on two adjustable parameters known as thresholds [21]. The Hard Threshold (HT) defines the absolute limit for a given measured parameter; data are transmitted only when the sensed value equals or exceeds this limit. The Soft Threshold (ST) determines the minimal variation of the measured value required to trigger a new transmission. In practice, HT prevents continuous reporting of stable environmental conditions, while ST ensures that only significant

deviations are communicated. Both threshold values are application-dependent and must be carefully selected to achieve an optimal trade-off between energy efficiency and data fidelity.

However, the reduction of transmitted packets inevitably leads to sparser datasets at the receiver side. Although interpolation techniques can reconstruct missing values to some extent, the resulting approximation may not always capture rapid or irregular environmental fluctuations accurately. Therefore, determining appropriate threshold parameters is a crucial aspect of system design. In this research, four algorithmic approaches (Fig. 2) were implemented and tested to evaluate their impact on energy savings and data accuracy.

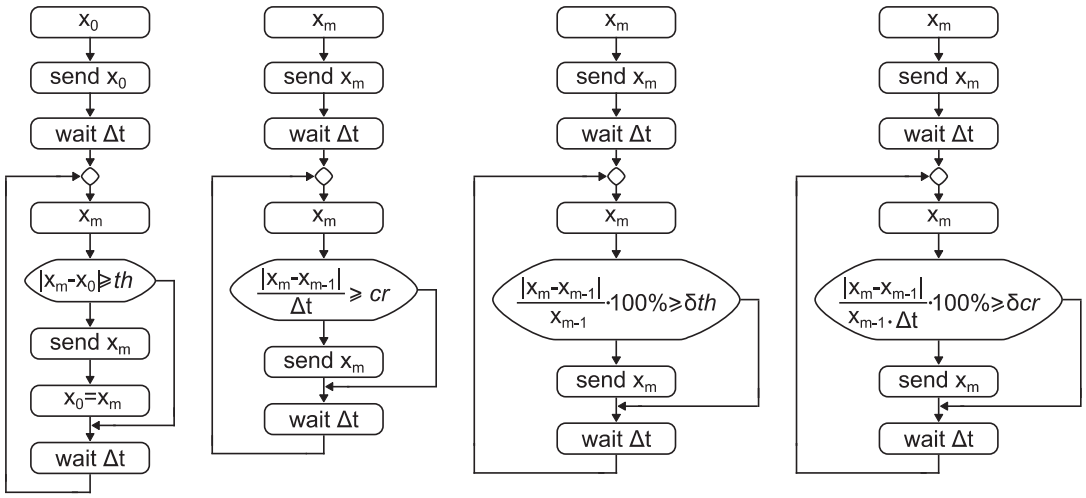

Figure 2 The algorithms implemented in the multi-sensor node

The first algorithm is based on the absolute difference between the most recent measurement and the previously transmitted value. Data transmission occurs only if this difference exceeds a predefined threshold (*th*). After each valid transmission, the node enters a low-power sleep mode for a specified duration (Δt) before acquiring new data.

The second algorithm introduces a rate-of-change criterion, where the node calculates the ratio between the absolute difference of consecutive measurements and the elapsed time interval. Transmission is initiated only when this rate exceeds a preset change rate (*cr*).

The third algorithm relies on the relative change of consecutive measurements, expressed as δth. Data are sent if the relative deviation surpasses this threshold.

Finally, the fourth algorithm combines the previous two approaches, using a hybrid criterion (δcr) that simultaneously considers both relative and time-dependent changes in the measured signal.

These algorithms collectively form the communication and energy-management framework of the proposed LoRa-TEEN-based monitoring system. By selectively transmitting only relevant information and employing adaptive thresholds, the system achieves a substantial reduction in communication overhead and energy consumption, extending the operational lifetime of each node without compromising environmental data reliability.

4 DATA ANALYSIS AND EVALUATION METHODS

To evaluate the performance of the proposed communication algorithms, a series of field experiments was conducted at the archaeological site "Mediana" in Niš, Serbia. The sensor node, equipped with the described multi-sensor platform, was installed in an outdoor environment and operated continuously for a period of seven days. Measurements were recorded every five minutes, resulting in a total of 2427 transmitted packets during the reference test period.

Each of the four transmission algorithms described in Section 3 was applied to the collected datasets under different threshold configurations. The purpose of this analysis was to quantify the trade-off between reduced transmission frequency - hence lower energy consumption - and the accuracy of the reconstructed environmental data at the receiver side. After each algorithm was applied, the reduced set of transmitted samples was interpolated to reconstruct a full-resolution signal, which was then compared with the original dataset recorded during the reference period.

Two principal analytical metrics were used to assess the degree of similarity between the reconstructed and original signals: Pearson's correlation coefficient (*r*) [22] and Root Mean Square Error (RMSE). The correlation coefficient quantifies the linear relationship between two data sequences and varies between 0 and 1, where a value of 1 denotes a perfect positive correlation. It is mathematically defined as:

$$r_{X,Y} = \frac{N\sum_{n=1}^{N} X[n]Y[n] - \left(\sum_{n=1}^{N} X[n]\right)\left(\sum_{n=1}^{N} Y[n]\right)}{\sqrt{N\sum_{n=1}^{N} X^2[n] - \left(\sum_{n=1}^{N} X[n]\right)^2}\sqrt{N\sum_{n=1}^{N} Y^2[n] - \left(\sum_{n=1}^{N} Y[n]\right)^2}} \quad (1)$$

where $X[n]$ and $Y[n]$ represent individual samples of the reconstructed and original datasets, respectively.

The RMSE was used to quantify the average difference between the reconstructed and reference waveforms and is expressed as:

$$\text{RMSE} == \sqrt{\sum_{n=1}^{N} \frac{\left(X[n]-Y[n]\right)^2}{N}} \tag{2}$$

In addition, the Maximum Relative Error (MRE) was computed to characterize the largest individual deviation between two corresponding samples, providing insight into the worst-case difference between datasets:

$$\text{MRE} = \max\left\{\frac{X[n]-Y[n]}{X[n]}\cdot 100\%\right\} \tag{3}$$

These three metrics - correlation, RMSE, and MRE - jointly describe the accuracy and fidelity of the reconstructed signals.

4.1 Experimental Results

Each algorithm was tested across multiple threshold values to assess its effect on the number of transmitted packets, data accuracy, and overall energy consumption. As expected, increasing the threshold in any algorithm led to a progressive reduction in the number of data transmissions, which directly translated into lower energy usage. However, this benefit was accompanied by a modest loss in data resolution, manifested as lower correlation coefficients and higher reconstruction errors. Consequently, determining an optimal threshold value emerged as a critical factor for achieving the best trade-off between energy savings and data integrity.

The experiments included the monitoring of temperature, carbon monoxide (CO), and nitrogen dioxide (NO_2) concentrations, which are key parameters for assessing local air quality. The datasets were analyzed using both statistical and visual methods. As example, Tabs.1 to 4 summarize the results for CO, and Tabs. 5 to 8 for NO_2, illustrating how variations in the applied threshold influence the Pearson correlation coefficient (r) and Root Mean Square Error (RMSE). These two indicators served as the main quantitative measures of signal fidelity between the original and reconstructed datasets.

Table 1 Concentration of CO - the first algorithm

th	Pearson	RMSE	MRE	Packet
0,18	0,9943	0,1045	42,6634	436
0,2	0,9928	0,117	32,7082	376
0,22	0,9913	0,1274	32,7082	348
0,24	0,9907	0,1328	42,9858	312
0,26	0,9883	0,1485	42,9858	285

Table 2 Concentration of CO - the second algorithm

cr	Pearson	RMSE	MRE	Packet
0,1	0,9961	0,0856	32,7082	594
0,11	0,9951	0,0963	32,7082	500
0,12	0,9909	0,1307	32,7082	406
0,13	0,9879	0,1499	32,7082	355
0,14	0,9838	0,1735	32,7082	285

Table 3 Concentration of CO - the third algorithm

δth	Pearson	RMSE	MRE	Packet
0,12	0,993	0,1249	39,8185	509
0,13	0,9927	0,1261	39,8185	470
0,14	0,9904	0,1483	39,8185	427
0,15	0,9894	0,1552	39,8185	403
0,16	0,9879	0,1664	39,8185	363

Table 4 Concentration of CO - the fourth algorithm

δcr	Pearson	RMSE	MRE	Packet
0,0525	0,9946	0,1107	29,9314	940
0,0575	0,9938	0,12	29,9314	854
0,0625	0,9909	0,1418	29,9314	797
0,065	0,9895	0,1547	29,9314	758
0,0725	0,9843	0,2012	37,017	650

Table 5 Concentration of NO_2 - the first algorithm

th	Pearson	RMSE	MRE	Packet
0,17	0,9928	0,1066	7,171	517
0,19	0,991	0,1189	8,9204	447
0,21	0,9901	0,1251	8,6981	408
0,23	0,9885	0,1347	9,1567	363
0,25	0,9875	0,1407	9,1567	334

Table 6 Concentration of NO_2 - the second algorithm

cr	Pearson	RMSE	MRE	Packet
0,105	0,995	0.0889	7.171	726
0,115	0,9934	0.1017	8.3614	618
0,125	0,9912	0.1179	8.8935	524
0,135	0,9884	0.1355	9.7716	457
0,145	0,9842	0.1577	12.2921	378

Table 7 Concentration of NO_2 - the third algorithm

δth	Pearson	RMSE	MRE	Packet
0,025	0,9954	0,0856	7,0934	672
0,03	0,9932	0,1044	7,3545	539
0,035	0,9911	0,1187	7,3236	440
0,04	0,9884	0,1367	8,6981	388
0,045	0,9869	0,1448	9,0807	339

Table 8 Concentration of NO_2 - the fourth algorithm

δcr	Pearson	RMSE	MRE	Packet
0,021	0,9934	0,1022	7,0595	637
0,022	0,9921	0,1118	7,171	586
0,023	0,9911	0,1185	7,3039	538
0,024	0,9897	0,1273	8,8935	493
0,025	0,9881	0,1369	8,8935	454

For air-quality applications, maintaining a correlation coefficient above 0.99 and an RMSE below 1 was defined as the minimum acceptable standard for reliable environmental data reconstruction. Within this range, the first algorithm, based on the absolute difference between consecutive measurements, achieved the most favorable balance between transmission reduction and accuracy preservation. This approach proved robust against small signal fluctuations and short-term noise, triggering data transmission only when a measurable change in environmental conditions occurred. Consequently, the algorithm yielded high correlation with significantly fewer transmissions compared to other methods, confirming its superior energy efficiency and practical applicability for continuous environmental monitoring.

In contrast, algorithms based on rate of change and relative difference displayed slightly higher variability in correlation values, particularly during periods of rapid environmental variation. Although these algorithms achieved further reductions in transmission count, they also introduced larger deviations from the original dataset, suggesting their suitability primarily for applications with slow-changing parameters. The hybrid algorithm, which combined time- and value-based thresholding, provided intermediate results - offering flexible adaptability at the expense of slightly higher computational complexity.

A representative comparison between the original and reconstructed signals is presented in Fig. 3. The black line

represents the original measured signal, while the red dots denote the reconstructed values generated by the first algorithm. The visual correspondence between the two waveforms confirms the quantitative analysis, indicating only minor deviations around transient peaks. This demonstrates that the algorithm successfully preserves the temporal trend and amplitude of environmental variations while drastically reducing communication frequency.

Overall, the experimental results confirm that the integration of TEEN-based adaptive thresholding with LoRa communication enables significant energy savings without compromising measurement quality. The first algorithm, due to its simplicity and robustness, can be considered the optimal configuration for practical deployment in long-term air-quality monitoring networks. It effectively balances energy consumption and information reliability, allowing autonomous, low-power nodes to operate for extended periods without human intervention or external power sources.

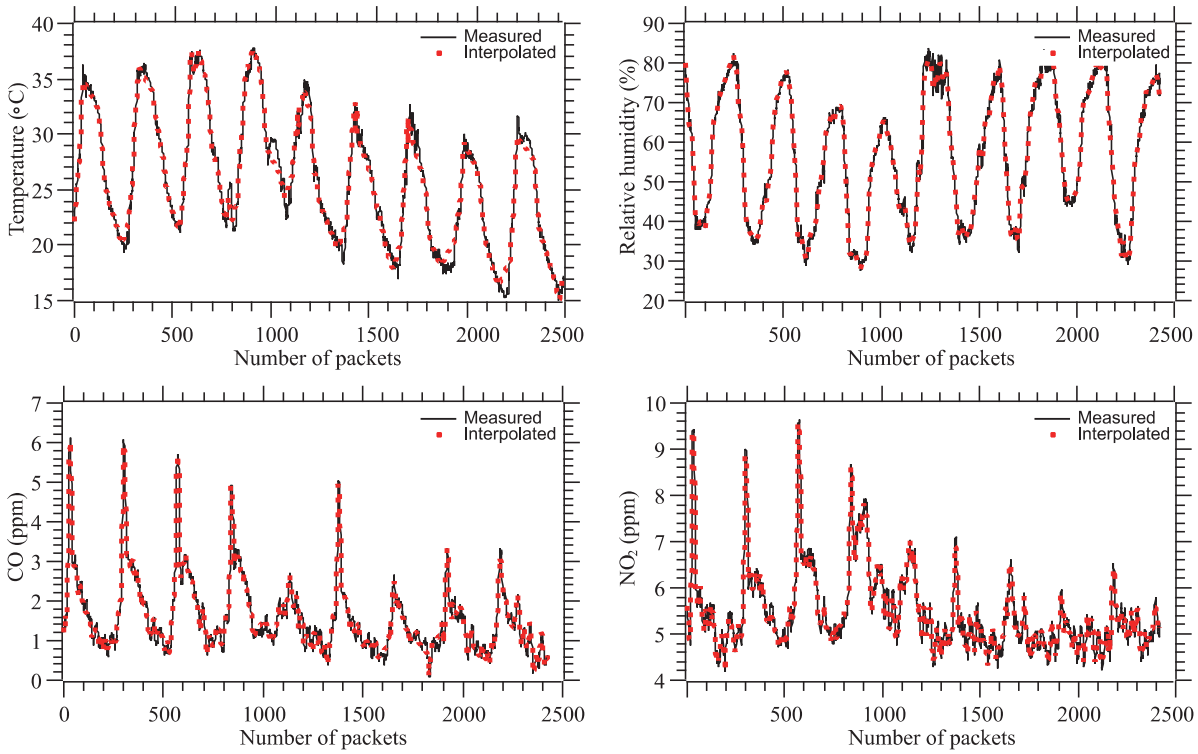

Figure 3 The waveforms comparison

4.2 Energy Consumption Evaluation

In wireless sensor networks, energy consumption during communication is often the dominant factor determining system lifetime. To quantify the energy efficiency of the proposed LoRa-TEEN framework, the transmission energy requirements were evaluated using both continuous and event-driven modes of operation. Each transmitted packet contained four measured parameters: temperature, humidity, CO, and NO_2. Every parameter occupied 6 bytes of data - one byte reserved for the parameter identifier and five bytes for the measured value - resulting in a total packet size of 24 bytes per transmission

Based on measurements and LoRa transceiver specifications, the energy required to transmit one packet was estimated at 54.432 mJ, corresponding to approximately 13.608 mJ per individual parameter. This value includes the combined consumption of the transceiver, microcontroller, and peripheral circuits during the active transmission window. Under continuous transmission mode, where data from all parameters are sent every five minutes, a total of 2427 packets were transmitted during the experimental period. The resulting cumulative energy consumption was approximately 132.106 J, representing the reference baseline for energy comparison.

When the first adaptive algorithm - based on the absolute difference - was applied, the number of transmitted packets decreased significantly. During the same observation period, the node transmitted 1521 parameter values (125 for temperature, 594 for humidity, 394 for CO, and 408 for NO_2). The total energy expenditure dropped to 20.697 J, representing a reduction of approximately 85% compared with continuous operation. This result demonstrates the clear impact of event-driven communication and threshold-based logic on extending the operational lifetime of autonomous sensor nodes

To further illustrate the effect of this reduction, consider a typical field deployment powered by a 3.7 V, 2200 mAh lithium-ion battery (8.14 Wh, or ≈29300 J). Under continuous transmission conditions, the system would theoretically operate for around 220 hours (≈9 days) before battery depletion. In contrast, when operating under the proposed adaptive algorithm, energy consumption is reduced by a factor of six, extending the battery lifetime to approximately 55 days on a single charge.

Additionally, the node incorporates a photovoltaic charging system, which replenishes the battery during daylight hours. Under moderate solar radiation (about 5 hours of effective sunlight per day), the solar cell provides sufficient energy not only to offset daily consumption but

also to maintain a positive energy balance, enabling indefinite operation under normal outdoor conditions. The hybrid energy-harvesting and management system thus ensures full autonomy and eliminates the need for manual maintenance or battery replacement, even in long-term monitoring periods.

The detailed energy distribution analysis also showed that data transmission accounts for approximately 70-75% of the total power budget, while sensing and processing consume less than 20%, and idle-state leakage currents contribute the remainder. Therefore, minimizing transmission frequency through adaptive thresholding directly results in substantial energy conservation. Furthermore, LoRa modulation was confirmed to be particularly advantageous for this purpose, as it maintains long communication ranges while operating at power levels below 100 mW.

In conclusion, the integration of TEEN-based threshold control with LoRa long-range communication and solar-assisted energy supply proved highly effective in achieving sustainable energy management. The proposed configuration ensures prolonged operational autonomy of wireless sensor nodes, providing a foundation for scalable, maintenance-free air-quality monitoring networks capable of multi-month or even year-long deployments.

5 DISCUSSION

The obtained results confirm that the integration of adaptive threshold algorithms within the TEEN-LoRa framework provides an effective compromise between energy efficiency and data accuracy in long-term air-quality monitoring. By reducing transmission frequency according to predefined threshold parameters, the system achieves considerable energy savings while preserving a high correlation with reference data.

An inverse relationship was observed between the applied threshold value and both the number of transmitted packets and data fidelity. For moderate thresholds, Pearson's correlation coefficients remained above 0.99 with RMSE < 1, even when the number of transmissions decreased by an order of magnitude. This demonstrates that the system can accurately capture environmental trends while drastically lowering energy consumption.

Among the four algorithms tested, the absolute-difference algorithm proved most effective, transmitting data only when the change between consecutive measurements exceeded a set limit. This simple event-based rule efficiently filters insignificant fluctuations and maintains high data integrity. The approach reduced total energy use by about 85 %, extending the operational lifetime of battery- or solar-powered nodes from weeks to several months.

No significant packet losses or synchronization issues occurred during continuous operation, confirming the robustness of LoRa communication under outdoor conditions. Compared to LEACH and PEGASIS routing schemes, TEEN demonstrated better energy distribution and responsiveness by activating nodes only during significant environmental variations.

While the threshold-based approach provides substantial energy savings, it may lead to the loss of fine-grained information and reduced sensitivity to sudden changes in pollutant levels, particularly when rapid fluctuations occur between sampling intervals. Future work will focus on machine-learning-based adaptive thresholds and predictive analytics to further enhance the precision and sustainability of IoT air-quality systems.

6 CONCLUSION

This work presented an energy-efficient multisensor platform for air-quality monitoring based on LoRa communication and the TEEN routing protocol. The system integrates electrochemical CO and NO_2 sensors, a low-power PIC18F45K22 microcontroller, and a photovoltaic power subsystem, enabling autonomous operation under outdoor conditions.

The proposed communication framework employs adaptive, threshold-based algorithms that significantly reduce the frequency of wireless transmissions. Experimental results demonstrated that the first algorithm -based on absolute measurement difference - achieved correlation coefficients above 0.99 with an 85% reduction in total energy consumption. This balance between measurement accuracy and energy efficiency confirms the suitability of TEEN-LoRa integration for long-term environmental monitoring.

The findings highlight that intelligent, event-driven transmission can extend the lifetime of low-power wireless nodes while maintaining high data fidelity. The developed architecture provides a scalable and sustainable basis for future air-quality monitoring networks and smart-city applications

The present work focused on a single-node WSN implementation to precisely examine the behavior of adaptive threshold algorithms under real environmental conditions. While this approach provides clear insight into the energy-accuracy trade-off, a multi-node deployment may exhibit additional phenomena such as congestion, packet collision, cluster-level delays, or routing instability. Therefore, further studies involving larger network topologies are required to fully assess the scalability and robustness of the proposed communication framework.

Acknowledgements

This work was supported by the Ministry of Science, Technological Development and Innovation of the Republic of Serbia (grant number 451-03-137/2025-03/200102).

7 REFERENCES

[1] Zhang, X., Han, L., Wei, H., Tan, X., Zhou, W., & Li, W. (2022). Linking urbanization and air quality together: A reviewand a perspective on the future sustainable urban development. *Journal of Cleaner Production*, *2022*, 130988. https://doi.org/10.1016/j.jclepro.2022.130988

[2] Šabanovič, A., Matijošius, J., Marinković, D., Chlebnikovas, A., Gurauskis, D., Gutheil, J. H., & Kilikevičius, A. (2025). Experimental setup and machine learning-based prediction model for electro-cyclone filter efficiency: Filtering of ship particulate matter emission. *Atmosphere*, *16*(1), 103. https://doi.org/10.3390/atmos16010103

[3] McCarron, A., Semple, S., Braban, C. F. et al. (2023). Public engagement with air quality data: Using health behaviour

change theory to support exposure-minimising behaviours. *Journal of Exposure Science & Environmental Epidemiology*, *33*, 321-331. https://doi.org/10.1038/s41370-022-00449-2

[4] Abera, A., Friberg, J., Isaxon, C., Jerrett, M., Malmqvist, E., Sjöström, C., Taj, T., & Vargas, A. M. (2021). Air quality in Africa: Public health implications. *Annual Review of Public Health*, *42*, 193-210. https://doi.org/10.1146/annurev-publhealth-100119-113802

[5] Camarillo-Escobedo, R., Flores, J. L., Marin-Montoya, P., García-Torales, G., &Camarillo-Escobedo, J. M. (2022). Smart multi-sensor system for remote air quality monitoring using unmanned aerial vehicle and LoRaWAN. *Sensors*, *22*(5), 1706. https://doi.org/10.3390/s22051706

[6] Zhang, H., Srinivasan, R., &Ganesan, V. (2021). Low-cost, multi-pollutant sensing system using Raspberry Pi for indoor air quality monitoring. *Sustainability*, *13*(1), 370. https://doi.org/10.3390/su13010370

[7] Felici-Castell, S., Segura-Garcia, J., Perez-Solano, J. J., Fayos-Jordan, R., Soriano-Asensi, A., &Alcaraz-Calero, J. M. (2023). AI-IoT low-cost pollution-monitoring sensor network to assist citizens with respiratory problems. *Sensors*, *23*(23), 9585. https://doi.org/10.3390/s23239585

[8] Johnston, S. J., Basford, P. J., Bulot, F. M. J., Apetroaie-Cristea, M., Easton, N. H. C., Davenport, C., Foster, G. L., Loxham, M., Morris, A. K. R., & Cox, S. J. (2019). City scale particulate matter monitoring using LoRaWAN based air quality IoT devices. *Sensors*, *19*(1), 209. https://doi.org/10.3390/s19010209

[9] Parra-Medina, F. D., Vélez-Guerrero, M. A., & Callejas-Cuervo, M. (2024). Low-cost solution for air quality monitoring: Unmanned aerial system and data transmission via LoRa protocol. *Sustainability*, *16*(22), 10108. https://doi.org/10.3390/su162210108

[10] Hassan, A. K., Saraya, M. S., Ali-Eldin, A. M. T., & Abdelsalam, M. M. (2024). Low-cost IoT air quality monitoring station using cloud platform and blockchain technology. *Applied Sciences*, *14*(13), 5774. https://doi.org/10.3390/app14135774

[11] Microchip Technology Inc. (2010-2021). *Low-power, high-performance microcontrollers with XLP technology, PIC18(L)F2X/4XK22*.

[12] Honeywell. (2015). *Honeywell Humid Icon™ digital humidity/temperature sensors HIH6100 series*.

[13] SPEC Sensors. (2017). *3SP NO2 5F*.

[14] SPEC Sensors. (2017). *3SP CO 1000*.

[15] Texas Instruments. (2014). *LMP91000 sensor AFE system: Configurable AFE potentiostat for low-power chemical-sensing applications*.

[16] Kanoun, O., Bradai, S., Khriji, S., Bouattour, G., El Houssaini, D., Ben Ammar, M., Naifar, S., Bouhamed, A., Derbel, F., & Viehweger, C. (2021). Energy-aware system design for autonomous wireless sensor nodes: A comprehensive review. *Sensors*, *21*(2), 548. https://doi.org/10.3390/s21020548

[17] Ramalingam, I. & Sankaran, R. A. (2018). Lifetime maximization of wireless sensor networks for a fault diagnosis system using LEACH protocol. *Tehnički vjesnik - Technical Gazette*, *25*(3). https://doi.org/10.17559/tv-20170213053711

[18] Juwaied, A., Jackowska-Strumillo, L., & Sierszeń, A. (2025). Enhancing clustering efficiency in heterogeneous wireless sensor network protocols using the k-nearest neighbours algorithm. *Sensors*, *25*(4), 1029. https://doi.org/10.3390/s25041029

[19] Lim, S. & Shin, B. (2024). A novel chain formation scheme for balanced energy consumption in WSN-based IoT network. *Tehnički vjesnik*, *31*(2), 525-533. https://doi.org/10.17559/TV-20220706031646

[20] Khan, A. R., Rakesh, N., Bansal, A., &Chaudhary, D. K. (2015). Comparative study of WSN protocols (LEACH, PEGASIS and TEEN). *2015 Third International Conference on Image Information Processing (ICIIP)*, 422-427. https://doi.org/10.1109/ICIIP.2015.7414810

[21] Manjeshwar, A. & Agrawal, D. P. (2001). TEEN: A routing protocol for enhanced efficiency in wireless sensor networks. *Proceedings of the 15th International Parallel and Distributed Processing Symposium (IPDPS)*, 2009-2015. https://doi.org/10.1109/IPDPS.2001.925197

[22] Kundrata, J., Fujimoto, D., Hayashi, Y., & Barić, A. (2020). Comparison of Pearson correlation coefficient and distance correlation in correlation power analysis on digital multiplier. *2020 43rd International Convention on Information, Communication and Electronic Technology (MIPRO)*, 146-151. https://doi.org/10.23919/MIPRO48935.2020.9245325

Contact information:

LJUBOMIR VRAČAR, Associate Professor
Faculty of Electronic Engineering, University of Niš,
18000 Niš, Serbia
E-mail: ljubomir.vracar@elfak.ni.ac.rs

JONAS MATIJOŠIUS, Associate Professor,
Mechanical Science Institute,
Vilnius Gediminas Technical University-VILNIUS TECH,
Plytinėsst. 25, LT-10105 Vilnius, Lithuania
E-mail: jonas.matijosius@vilniustech.lt

MILAN STOJANOVIĆ, Teaching Assistant, PhD student
Faculty of Electronic Engineering, University of Niš,
18000 Niš, Serbia
E-mail: milan.stojanovic@elfa.ni.ac.rs

ARTŪRAS KILIKEVIČIUS, Professor,
Mechanical Science Institute,
Vilnius Gediminas Technical University-VILNIUS TECH,
Plytinėsst. 25, LT-10105 Vilnius, Lithuania
E-mail: arturas.kilikevicius@vilniustech.lt

MILOŠ MILOVANČEVIĆ, Associate Professor
(Corresponding author)
Faculty of Mechanical Engineering, University of Niš,
18000 Niš, Serbia
E-mail: milos.milovancevic@masfak.ni.ac.rs